PERGAMON

Planetary and Space Science 48 (2000) 775–783

Planetary and Space Science

www.elsevier.nl/locate/planspasci

Thermal plasma composition in Saturn's magnetosphere

W.-H. Ip

Institute of Astronomy, National Central University, Chung Li 320, Taiwan

Received 10 July 1998; received in revised form 25 November 1999; accepted 7 January 2000

Abstract

A brief description is given to the composition of the thermal ions in the Saturnian magnetosphere with the neutral gas cloud as the main source. It is predicted that, if the neutral cloud density peaks near Enceladus' orbit with a total number density of the water-group neutrals reaching 10^4 cm^{-3}, the molecular ions like OH^+ and H_2O^+ could be as abundant as O^+ throughout the Saturnian magnetosphere. At the same time, a significant amount of H_3O^+ and O_2^+ ions can be found in the region with $L < 5$. The composition of the Saturnian plasma could therefore be far more complex than previously thought.

1. Introduction

Even though the last closeup observations of the Saturnian system were by the Voyager spacecraft in 1980 and 1981, there is a steady stream of exciting new observations of the physical phenomena of this ringed planet from ground-based and space-born observatories over the last few years. In some areas, the new measurements have completely supplanted our old ideas. One example is the distribution of neutral gas cloud which has now been found to be extremely dense by the Hubble Space Telescope observations (Shemansky and Hall, 1992; Shemansky, 1998). Its impact on the composition and dynamics of the Saturnian magnetosphere is still to be carefully assessed. In this work, we will examine several major ingredients in the neutral cloud origin of the magnetospheric plasma. These include source (Section 2), composition (Section 3), and configuration (Section 4).

2. Source

It is useful to compare the Saturnian magnetosphere with the Jovian magnetosphere. Both planets have similar rotational periods ($P = 9$ h 55.5 min for Jupiter and 10 h 39 min for Saturn) so that for both of them the corotational electric field tends to dominate the solar wind convective electric field in shaping the magnetospheric plasma motions (Brice and Ioannidis, 1970; Mendis and Axford, 1974; Vasyliunas, 1983). Jupiter's large magnetic dipole moment (equatorial magnetic field $B_{eq} = 4.2$ Gauss) and the presence of a large population of hot plasma help to inflate the Jovian magnetosphere into a disc-like structure dominated by a strong current sheet near the magnetic equator (Acuna et al., 1983; Krimigis and Roelof, 1983). With a smaller magnetic moment ($B_{eq} = 0.22$ Gauss) and much reduced level of energetic charged particle population the Saturnian magnetosphere is less dynamic. For example, the pronounced 10-h periodicity observed in the particle fluxes of the Jovian magnetosphere is absent in the Saturnian magnetosphere. This can be partly traced to the near-zero tilt of Saturn's dipole axis. Furthermore, because of the absorption effect of the main rings between 1.3 and $2.27R_S$ (Saturnian radius) and its weaker magnetic field, Saturn is not a strong emitter of synchrotron radiation.

In spite of the large differences in the energetic particle populations, Jupiter and Saturn share the distinc-

E-mail address: wingip@joule.phy.ncu.edu.tw (W.H. Ip).

0032-0633/00/$ - see front matter
PII: S0032-0633(00)00036-2

tion that their satellites are important sources of the magnetospheric thermal plasma. Because of its active volcanism, Io is emitting a large amount of neutral and ionized (SO_2) gas via ion sputtering at a mass loss rate of $\dot{M} \approx 1 - 2 \times 10^6$ g/s into the Jovian magnetosphere (Bagenal, 1992). As a result of thermal sublimation and surface sputtering by energetic ions, Europa, Ganymede and Callisto are also sources of neutral gas of water composition. Europa in particular could be a second most important plasma source in the Jovian magnetosphere with a mass loss rate of 2×10^5 g/s (Johnson et al., 1982; Ip, 1996; Ip et al., 1998; Saur et al., 1998).

In the case of the Saturnian satellites, it is not certain whether thermal sublimation (because of low surface temperature) and ion sputtering (because of low ion flux) could be as significant in ejecting gaseous material into the Saturnian magnetosphere. Impact vaporization by interplanetary meteoroids and/or collisional effect of the E-ring dust particles could instead play the leading role (Johnson et al., 1993; Shemansky et al., 1993; Shi et al., 1995). In view of the large number density (≈ 1000 cm^{-3}) of OH radical detected inside the orbit of Tethys by the Hubble Space Telescope, Shemansky (1998) estimated that the corresponding total number density of the water-group neutral gas (e.g., H_2O, OH, and O) could be as much as 3000 cm^{-3}. This new observational finding gives credence to the idea that it is the impact process of the E-ring particles at the rings, Enceladus and other icy satellites which produces such an extended neutral gas cloud (Hamilton and Burns, 1994; Ip, 1997).

Fig. 1 shows the number densities of the neutral gas molecules at the equatorial plane according to a neutral cloud model (Ip, 1997). In the computation, the parent molecule H_2O is assumed to have been emitted from the icy satellites as a result of E-ring particle impact and ion sputtering. After injection into circum-planetary orbits, the H_2O molecules will be dissociated or ionized by collisional interaction with the magnetospheric plasma and solar UV photons. The motion of the dissociation products, OH and O, are then traced so that the three-dimensional spatial extensions and number density variations of the water-group neutral gas can be constructed.

The relative abundance of H_2O, OH and O are approximations from the neutral cloud model calculations. The H atom, dissociated from H_2O is not explicitly included because it has relatively large excess energy and will hence not be confined in the same volume as the heavy neutrals. One neutral species of potential importance not discussed above has to do

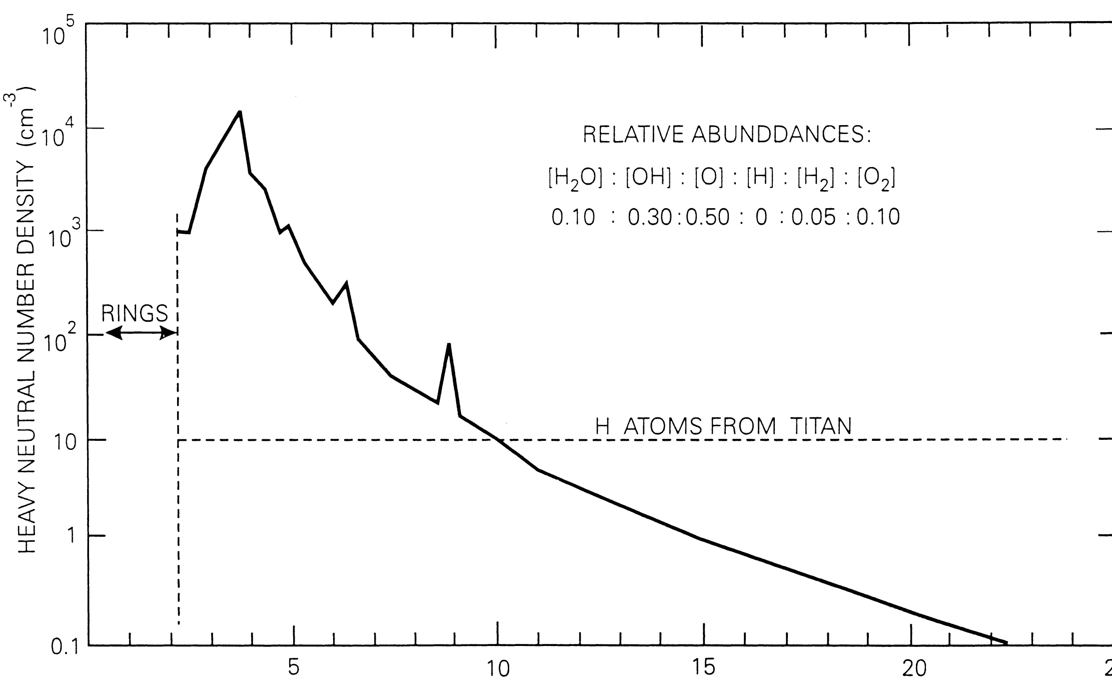

Fig. 1. A neutral gas cloud model derived by injecting H_2O molecules from individual icy satellites into the Saturnian magnetosphere. The density peaks feature the orbital positions of Enceladus ($L = 3.94$), Tethys ($L = 4.88$), Dione ($L = 6.25$), and Rhea ($L = 8.74$). The curve is for total number density at the equatorial plane averaged over all longitudes. The vertical scale height of the neutral cloud is assumed to be $H_n \sim 0.5\,R_S$. The relative abundances are: $[H_2O]$:[OH]:[O]:$[H_2]$:$[O_2] \sim 0.10$:0.30:0.50:0.05:0.10. The hydrogen atoms from Titan are assumed to have a constant number density in the Saturnian system.

with the oxygen molecule which can be effectively produced by ion sputtering of water ice or by recombination of the oxygen atoms at solid surface upon impacts (Johnson, 1990). In summary, the relative abundance of the neutral species from the icy satellites and ring particles are:

$$[H_2O]:[OH]:[O]:[O_2]:[H_2]:[H] = 0.10:0.30:0.50:0.10:0.05:0.0.$$

The ring system is supposed to produce an exosphere of its own because of continuous meteoroid impacts (Ip, 1984, 1995; Johnson et al., 1989; Pospieszalska and Johnson, 1991). The high Keplerian velocity in this radial interval ($\sim$1.3–2.27R_S) leads to a flat disc-like structure with a very small vertical scale height ($\sim 0.1 R_S$). Because of the effective absorption effect at impacts, the number density of the neutral gas emitted from the ring particles has a maximum value of about 100 cm^{-3} at the B ring (Ip, 1995). On the other hand, the neutral gas cloud associated with the icy satellites (i.e., Enceladus and Mimas) can support a far denser gas cloud system extending to the outer edge of the A ring, with the neutral particles in orbits not intercepting the rings. Such a dynamical relation can have important inference in the HST observations of the OH emission (Hall et al., 1996; Shemansky, 1998).

In addition to the neutral gas emitted from the rings and the icy satellites, Titan is also an important source for H atoms and H_2 molecules (McDonough and Brice, 1973; Broadfoot et al., 1981). We follow the analysis of the ultraviolet spectrometer observations on Voyager by Shemansky and Hall (1992) that the whole Saturnian system including the region inside $8R_S$ is filled with atomic hydrogen at a level of about 10 atoms cm^{-3}. The dispersal of Titan's atomic hydrogen torus is probably in part caused by the long-term dynamical effects of the solar radiation pressure and the large oblateness of the planet (Smyth and Marconi, 1993; Ip, 1996). Because of the large number density of the water-group neutrals in the inner magnetosphere, inter-particle collision will also facilitate orbital trapping of the inward-moving hydrogen atoms (D. E. Shemansky, private communication, 1998).

3. Composition

According to the Voyager observations of the thermal plasma environment of the Saturnian system (Bridge et al., 1981, 1982; Richardson and Sittler, 1990), the ion composition within $5R_S$ is dominated by heavy ions. Because of the limitation in mass resolution of the Voyager plasma instrument the exact composition of the corotating ions was not identified except that they are likely to be ion species related to the water group ions (i.e., O^+). With the neutral cloud composition model given above as input, we can in principle derive the ion composition by including the production rates and loss rates of different ions in a one-dimensional radial diffusion scheme. The system of photolytic reactions, electron impact ionization and dissociation, and ion-molecule reactions was given in Ip (1997). In addition, electron dissociative recombination processes are included in the present calculations. The electron collisional impact rates are sensitive to the ambient electron temperature (T_e) which radial variation is given in Fig. 2 according to Richardson (1995). Note the drop in T_e to about 1 eV at $L \approx 3.5$ which might be resulting from cooling effect of the dense neutral cloud in this region (Shemansky and Hall, 1992). It is possible that T_e falls even below 1 eV in which case the electron impact ionization rates will be significantly reduced while the electron dissociative recombination rates can be correspondingly enhanced. But before self-consistent thermal energy model calculations are carried out, the T_e profile from the Voyager measurements will be used as a general guide. By the same token, the radial variation of the ion temperatures (T_i) from Richardson (1995) will be adopted as input. The T_i values are in turn used to compute the plasma scale heights

$$H_i = \left(\frac{2kT_i}{3m_i\Omega^2}\right)^{1/2} \tag{1}$$

where m_i is the ion mass and Ω the angular rotation rate of Saturn. The vertical number density distribution of the ions can be described by

$$n_i(z) = n_0 \ \exp\left(\frac{-z^2}{H_i^2}\right) \tag{2}$$

where n_0 is the ion number density at the magnetic equator and z the corresponding vertical distance (Hill and Michel, 1976). If N_i is the number of the ith ion species in a magnetic flux shell per unit L, it can be defined as (Richardson and Siscoe, 1983):

$$N_i = 2\pi L R_S^2 \int_{-\infty}^{\infty} n_i(z)\ dz \approx 2\pi^{\frac{3}{2}} n_0 L^2 R_S^2 H_i \tag{3}$$

The ion species to be considered are the following: $H_2O^+ . H_3O^+$, OH^+, O_2^+, H^+, H_2^+ and H_3^+. Furthermore, the coupled radial diffusion equations of these ions can be written as:

$$\frac{\partial}{\partial t}(N_i L^2) = L^2 \frac{\partial}{\partial t}\left[\frac{D_{LL}}{L^2}\frac{\partial}{\partial L}(N_i L^2)\right] + Q_i - \Lambda_i \tag{4}$$

where Q_i and Λ_i are the source and sink terms, respectively, for the parameter N_iL^2. The radial diffusion coefficient D_{LL} is generally expressed in terms of $D_{LL} = D_o L^m$ with $m \approx 2$–3 if the magnetospheric diffusion process is controlled by atmospheric dynamo effect (Brice and McDonough, 1973; Mendis and Axford, 1973). In an analytical model of loss-free diffusion (i.e., $\Lambda_i = 0$), Barbosa (1990) found that a D_o value of 2×10^{-9} R_S^2/s could provide a good fit of the ion density profile if the source strength is taken to be $Q_i \approx 10^{26}$ ions/s. On the other hand, Richardson (1992) preferred a slower diffusion process with $D_o \sim 1$–3×10^{-10} R_S^2/s. Because the global variations of the ion density distributions are sensitive functions of the source and sink terms it is probably premature to select a specific D_o value in the model calculations. What we have opted to do is to test the radial diffusion model against a range of D_o values varying between 10^{-8} R_S^2/s and 10^{-10} R_S^2/s. This is to demonstrate how additional information on the diffusion rate can be obtained from the number densities and chemical composition of the thermal ions.

The time-dependent coupled diffusion equations are solved by the Crank–Nicholson scheme. One important assumption we have made in the computation is that the neutral densities (which are largely produced by meteoroid bombardment) and electron and ion temperatures at different radial distances remain fixed and are always the same for all runs irrespective of the ion and electron number densities (n_e). This is one limitation of the present model which needs to be addressed in future by updating the value of T_e and T_i and neutral gas model in succeeding time steps by considering the energy budgets of the magnetospheric plasma system. The results described here should therefore be viewed as a quick look with several of the important physical elements still to be implemented. Even so, some useful features can be found already in the present simplified models.

The quasi-stationary values of the flux tube content parameters N_iL^2 and ion number densities in the four different cases are summarized in Fig. 3. The general characteristic is that the Saturnian magnetospheric plasma is proton-rich in the outer region because of the Titan source. The radial distance (L_c) for transition to heavy-ion dominated composition depends on the diffusion rate. It varies from $L_c \approx 9$ for $D_o \approx 10^{-10}$ to $L_c \sim 13$ for $D_o \sim 10^{-8}$. The proton number density can be seen to be reduced inside the boundary of the ion temperature (scale height) jump. This is because of the enhanced production rate of H_3O^+ via $H^+ + H_2O^+$ in the neutral gas cloud. As with H_3O^+, the number density of the O_2^+ ion also peaks inside the orbit of Enceladus. This pattern is basically defined by the assumed radial distribution of the neutral gas.

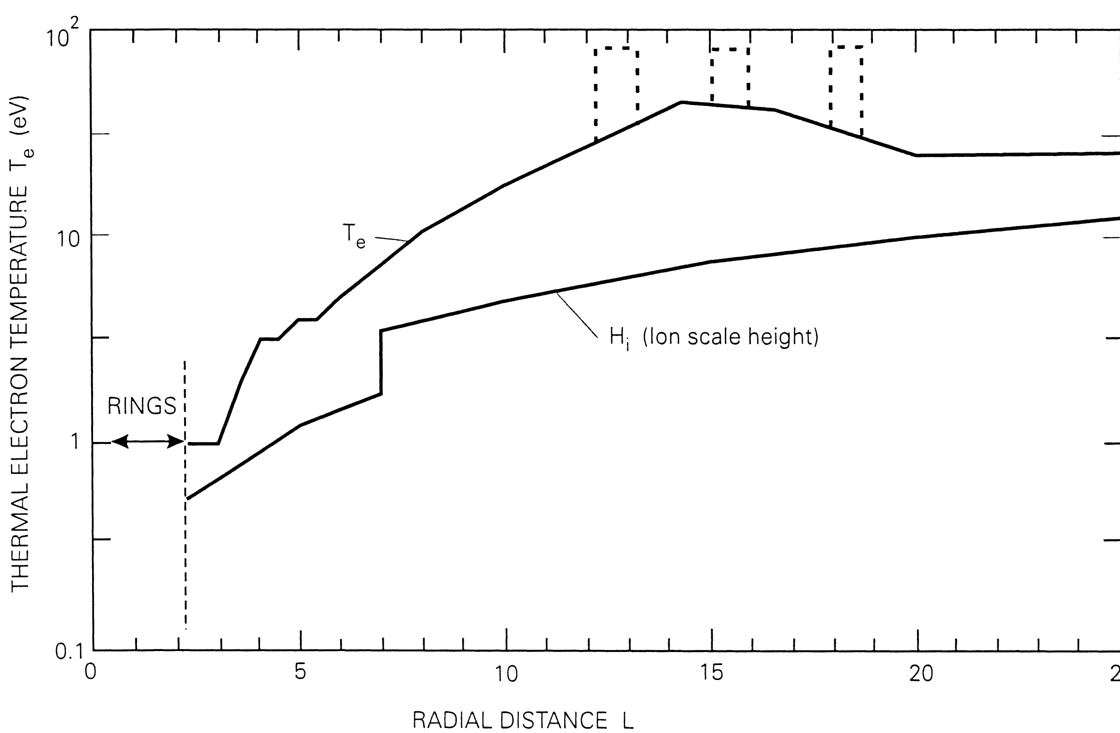

Fig. 2. The radial variations of the thermal electrons (T_e) and the ion scale height (H_i) used in the model calculations. The T_e values are from the Voyager measurements (Richardson, 1995). The dashed portion of the T_e profile is to indicate the presence of plasma bubbles. The discontinuity of the H_i value at $L \approx 7$ is to mimic the ion temperature observed by Voyager.

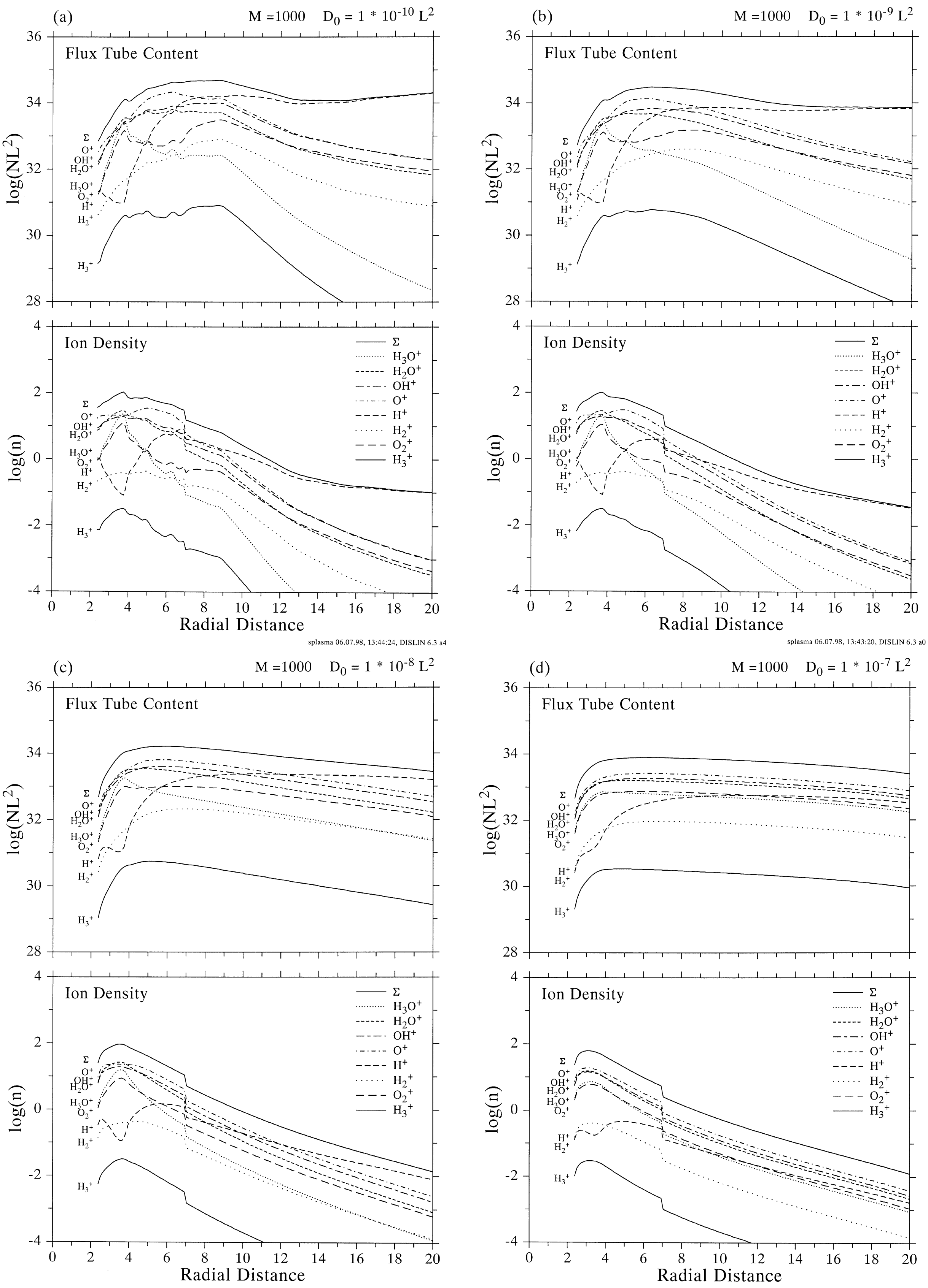

Fig. 3. The radial variations of the flux tube parameter $N_i L^2$ and the ion number density (n_i) at the equator for four different values of the radial diffusion coefficients (D_o): (a) 10^{-10}; (b) 10^{-9}; (c) 10^{-8} and (d) 10^{-7}, all in units of R_S^2/s.

One important diagnostic feature has to do with the abundance of atomic O^+ ion relative to the molecular ions like OH^+ and H_2O^+. For slow radial diffusion, the molecular ions would be significantly depleted inside the source region because of rapid electron dissociative recombination. On the other hand, the O^+ ions would not be as critically affected because of the much smaller electron dissociative recombination rate (e.g., $\alpha \sim 2 \times 10^{-7}$ cm^{-3}/s for H_2O^+ and $\alpha \sim 3 \times 10^{-12}$ cm^{-3}/s; see Schreier et al., 1993). As a consequence, the inner magnetosphere would become enriched in O^+ for $D_o < 10^{-10}$. However, the molecular ions could be effectively purged to the outer magnetosphere given a fast diffusion rate. Thus a large diffusion coefficient with $D_o \sim 10^{-9}$–10^{-8} will tend to increase the relative abundance of the molecular ions even though the absolute value of the total ion number density would become smaller because of diffusive loss.

It is to be understood that such theoretical models are still at the early stage of development. Besides the uncertainties in the radial transport rate and energy budget, one major unknown is the detailed radial distributions of the neutral gas species. The issue on whether ion sputtering or meteoroid impact is the dominant source mechanism is still unsolved. In a recent work, Richardson et al. (1998) has produced a composition model using a somewhat different numerical approach. These authors favored a sputtering source for the neutral gas cloud. The most important difference from our present calculations is that a relatively flat density profile [n(OH) $\approx$ 300 cm^{-3} at $L \approx 3$–50 cm^{-3} at $L \approx 10$ and n(O) $\approx$ 100 cm^{-3} through the same radial interval] is invoked in Richardson's model. The neutral cloud model used in the present work has a peak number density ($\approx 10^4$ cm^{-3}) at the orbit of Enceladus because of the collisional impact effect of the E-ring particles. This neutral density peak is followed by a relatively steep curve with total number density of the water-group neutrals decreasing to about 10 cm^{-3} at $L \approx 10$. An intercomparison and, possibly, combination of both approaches would improve our understanding of the origin of the Saturnian magnetospheric plasma. For example, as will be discussed later, the ballistic transport of the neutral particles from electron dissociative recombination or charge transfer in the inner plasma torus could redistribute oxygen atoms and other neutrals to large radial distances at $L > 10$.

4. Configuration

The formulation of the one-dimensional radial diffusion equation is applicable to an azimuthally symmetric system. However, the measurements by Voyager 1 and 2 spacecraft showed that significant longitudinal asymmetry existed in the structure of the plasma disc. Firstly, both inbound passes near noon detected a plasma density discontinuity at $L \approx 15$ (Sittler et al., 1983). The plasma inside this boundary was characterized by a cold electron temperature ($T_e < 40$ eV) and high number density. On the contrary, the plasma outside had large electron temperature ($T_e \approx 100$ eV) and low number density (Richardson, 1995). For $L > 15$, several dense plasma clouds were found by Voyager 2 as if they had been detached from the outer edge of the dense plasma disc.

Goertz (1983) suggested that these plasma clouds might have been produced by the Kelvin–Helmhotz instability at the turbulent boundary layer. Another possibility is that these plasma clouds were torn away from the plasma disc because of the time variation of the solar wind convective electric field. An enhanced interplanetary electric field could lead to a temporary exchange of the thermal plasma from a corotational flow configuration to a planetary wind outflow. Fig. 4 is a sketch of the different flow regimes by a simple

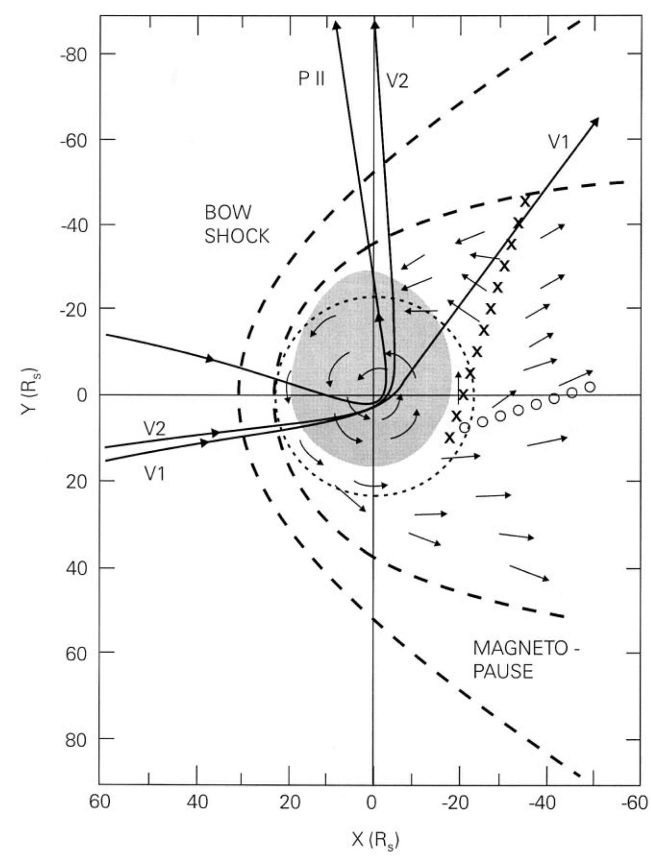

Fig. 4. A schematic view of the two-dimensional structure of the corotating plasma disc. The magnetospheric flow pattern is scaled from the Vasyliunas model for the Jovian magnetosphere. The postulated spatial shift of the plasma disc is caused by the presence of a dawn-to-dusk electric field generated by a planetary wind in the magnetospheric tail.

scaling of the Vasyliunas model for the Jovian magnetosphere (Vasyliunas, 1983) to the Saturnian case. It is suggested here that the limitation of the extension of the plasma disc on the sunward side could be related to the bifurcation of the flow patterns in the nightside magnetosphere.

The tailward escape of the magnetospheric plasma should drive a dawn-to-dusk cross tail electric field similar to what has been inferred at Jupiter (Barbosa and Kivelson, 1983; Ip and Goertz, 1983). The drifting of the corotating plasma in the displaced L shell could in principle created an elongated plasma disc with the apex pointing towards local dawn possibly reaching the magnetopause. Such contact could also be conductive to the detachment of plasma clouds by way of Kelvin–Helmhotz instability as proposed by Goertz (1983).

The schematic picture depicted in Fig. 4 shows that during its orbital motion around Saturn, Titan moves through different plasma regions. Near the dawn side, Titan is interacting with the dense plasma disc. But at local noon and the dusk side, Titan is moving in the area where effective mass loss will take place. Near the midnight sector, Titan could be experiencing a tailward flow at 90° from the corotational motion. As a result, the ionospheric wake of Titan could swing by a large angle in this region. Another important consequence is that the ionospheric plasma emitted from Titan's exosphere will be lost for a large fraction of the orbital time without being incorporated into the plasma disc. The same might be true for the nitrogen ions created in its gas torus.

5. Discussion

It is possible that the electron temperature at $L < 4$ is much smaller than 1 eV as a result of collisional cooling by the dense neutral gas cloud (Shemansky and Hall, 1992). Consequently, the ion number density could be kept low in this region even though the neutral gas density is relatively high ($\approx 10^4$ cm^{-3}). The situation is somewhat similar to the structure of the cometary ionosphere of Comet Halley in which the inner region of cold electron temperature ($T_e \approx 500$ K) is surrounded by a plasma of high electron temperature ($T_e \approx 3 \times 10^4$ K) at which boundary the ion number density varies by a factor of 3 to 4 (Eberhardt and Krankowsky, 1995; Gan and Cravens, 1990; Ip, 1994). The density jump is basically produced by the much higher electron dissociative recombination rate of molecular ions in the inner ionosphere caused by the lower electron temperature therein. At Saturn, it is very likely that the innermost magnetospheric region between the outer edge of the ring system and $L \approx 4$ is characterized by photoionization and the outer part with $L > 4$ by electron impact ionization. As indicated in Fig. 3, the ion composition of the photochemical region should be dominated by molecular water-group ions whereas the outer zone by atomic oxygen ions.

The collisional interaction of the corotating ions with the neutral gas component and dissociative recombination of the water-group ions also leads to another interesting phenomenon. That is, depending on the initial velocity at creation the recombined neutral particles could be launched into circumplanetary orbits without being immediately lost to interplanetary space. Such ballistic transport effect could in principle inject neutral atoms and molecules (O, OH and H_2O) into the outer magnetosphere where no significant source of these neutral species is expected.

It is interesting to note that, because of our basic assumption of constant neutral density distributions and ionization time scales in all numerical runs, the ion density and composition distributions are nearly constant in the inner region of the Saturnian magnetosphere for a very wide range of the radial diffusion coefficients ($D_o \approx 10^{-10}$–10^{-8}). This apparent discrepancy can be resolved by comparing the ionization time scale of the neutral cloud and the corresponding dynamical (e.g., diffusion) time of the magnetospheric plasma within 4 R_S. At a temperature of about 1 eV, the ionization effect of the water-group neutrals are dominated by photoionization. At a solar distance of 10 AU the photoionization time of oxygen atoms is $\beta \sim 2 \times 10^{-9}$ s^{-1}. For a typical neutral density of $[O] \approx 500$ cm^{-3}, the photoionization time is therefore $t_i \sim 1/\beta$ [O] or 10^6 s. Taking the diffusion time scale to be $t_d \approx R_S^2/D \approx 1/D_o L^2$, we have $t_d \approx 1/9D_o$ if $L \approx 3$. Thus for D_o between 10^{-10} and 10^{-8}, $t_d \sim 10^7$–10^9 s. Since $t_i \gg t_d$, the ion density and composition of the magnetospheric plasma for $L \approx 3$–4 should therefore be mainly determined by the photoionization and chemistry instead of the radial diffusion effect. On the other hand, because of the rapid decrease of the neutral number density at $L > 7$, the diffusion process will become more and more important in determining the ion number density and ion composition. In other words, changing the transport rate in the inner magnetosphere makes little difference to the profile since transport is a minor loss mechanism compared to chemistry in the inner Saturnian magnetosphere.

Finally, it is important to point out that in our simplified treatment the scale heights of all ion species are assumed to be the same in the calculation of the source and sink terms. This scheme will be improved by taking into consideration the effect of the polarization electric field on the magnetic field-aligned distributions of different ions (Wilson and Waite, 1989; Maurice et al., 1997). As a result of the corotational centrifugal force, the heavy ions tend to concentrate towards the magnetic equatorial plane while protons would be evacuated from the low-latitude region because of the polarization electric field. Such a spatial separation of the light (H^+ and H_2^+) and heavy (OH^+ and H_2O^+) ions might be significant in the ion chemistry. A two-dimensional plasma model is therefore required to describe the full range of physical aspects in the Saturnian magnetosphere.

Acknowledgements

I thank D. E. Shemansky, R. E. Johnson, A. Kopp and J. D. Richardson for informative discussions, and Margit Steinmetz, F. Both and Apple Wang for assistance in preparing the manuscript. This work was supported in part by the German Aerospace Agency (DLR) and in part by the National Science Council Grant No. 88Afa0700296.

References

Acuna, M.H., Bahannon, K.W., Connerney, J.E.P., 1983. Jupiter's magnetic field and magnetosphere. In: Dessler, A.J. (Ed.), Physics of the Jovian Magnetosphere. Cambridge University Press, pp. 1–50.

Bagenal, F., 1992. Giant planet magnetospheres. Ann. Rev. Earth Planet. Sci. 20, 289–328.

Barbosa, D.D., 1990. Radial diffusion of low-energy plasma ions in Saturn's magnetosphere. J. Geophys. Res. 95, 17167.

Barbosa, D.D., Kivelson, M.G., 1983. Dawn-dusk electric field asymmetry of the Io plasma torus. Geophys. Res. Lett. 10, 210–213.

Brice, N.M., Ioannidis, G.A., 1970. The magnetospheres of Jupiter and Earth. Icarus 13, 173–183.

Brice, N.M., McDonough, T.R., 1973. Jupiter's radiation belts. Icarus 18, 206–219.

Bridge, H.S., Belcher, J.W., Lazarus, A.J., Olbert, S., Sullivan, J.D., et al., 1981. Plasma observations near Saturn: Initial results from Voyager 1. Science 212, 217–223.

Bridge, H.S., Bagenal, F., Belcher, J.W., Lazarus, A.J., McNutt, R.L., et al., 1982. Plasma observations near Saturn: Initial results from Voyager 2. Science 215, 563–570.

Broadfoot, A.L., Sandel, B.R., Shemansky, D.E., et al., 1981. Extreme ultraviolet observations from Voyager 1 encounter with Saturn. Science 212, 206–211.

Eberhardt, P., Krankowsky, D., 1995. The electron temperature in the inner Coma of comet P/Halley. Astron. Astrophys. 295, 795–806.

Gan, L., Cravens, T.E., 1990. Electron energetics in the inner coma of Comet Halley. J. Geophys. Res. 95, 6285–6303.

Goertz, C.K., 1983. Detached plasma in Saturn's turbulence layer. Geophys. Res. Lett. 10, 445–458.

Hall, D.T., Feldman, P.D., Holberg, J.B., McGrath, M.A., 1996. Fluorescent hydroxyl emissions from Saturn's ring atmosphere. Science 272, 516–518.

Hamilton, D.P., Burns, J.A., 1994. Origin of Saturn's E ring: self sustained, naturally. Science 264, 550–553.

Hill, T.W., Michel, F.C., 1976. Heavy ions from the Galilean satellites and the centrifugal distortion of the Jovian magnetosphere. J. Geophys. Res. 81, 4561–4565.

Ip, W.-H., 1984. The ring atmosphere of Saturn: Monte Carlo simulation of ring source models. J. Geophys. Res. 89, 8843–8849.

Ip, W.-H., 1994. On a thermodynamic origin of the cometary ion rays. Astrophys. J. 432, L143–L145.

Ip, W.-H., 1995. The exospheric systems of Saturn's rings. Icarus 115, 295–303.

Ip, W.-H., 1996. The asymmetric distribution of Titan's atomic hydrogen cloud as a function of local time. Astrophys. J. 457, 922–932.

Ip, W.-H., 1997. On the neutral cloud distribution in the Saturnian magnetosphere. Icarus 126, 42–57.

Ip, W.-H., Goertz, C.K., 1983. An interpretation of the dawn-dusk asymmetry of UV emission from the Io plasma torus. Nature 302, 232–233.

Ip, W.-H., Williams, D.J., McEntire, R.W., Mauk, B.H., 1998. Ion sputtering and surface erosion at Europa. Geophys. Res. Lett. 25, 829–832.

Johnson, R.E., 1990. Energetic Charged Particle Interactions with Atmospheres and Surfaces. Springer-Verlag, Berlin.

Johnson, R.E., Pospieszalska, M.K., Sittler Jr, E.C., Cheng, A.F., Lanzerotti, L.J., Sieveka, E.M., 1989. The neutral cloud and heavy ion inner torus at Saturn. Icarus 77, 311–329.

Johnson, R.E., Lanzerotti, L.J., Brown, W.L., 1982. Planetary applications of ion induced erosion of condensed-gas frost. Nucl. Intr. Meth. 198, 147–158.

Johnson, R.E., Grosjean, D.E., Jurak, S., Baragiola, R.A., 1993. Sputtering, still the dominant source of plasma at Dione? EOS Trans. 74, 569–573.

Krimigis, S.M., Roelof, E.C., 1983. Low-energy particle population. In: Dessler, A.J. (Ed.), Physics of the Jovian Magnetosphere. Cambridge University Press, pp. 106–156.

Maurice, S., Blanc, M., Prange, R., Sittler Jr, E.C., 1997. The magnetic-field-aligned polarization electric field and its effects on particle distribution in the magnetospheres of Jupiter and Saturn. Planet. Space Sci. 45, 1449–1465.

McDonough, T.R., Brice, N.M., 1973. New kind of ring around Saturn. Nature 242, 513.

Mendis, D.A., Axford, W.I., 1974. Satellites and magnetospheres of the outer planets. Ann. Rev. Earth Planet. Sci. 2, 419–474.

Pospieszalska, M.K., Johnson, R.E., 1991. Micrometeoritic erosion of main rings as a source of plasma in the inner Saturnian plasma torus. Icarus 93, 45–52.

Richardson, J.D., 1992. A new model for plasma chemistry and transport at Saturn. J. Geophys. Res. 97, 13705–13713.

Richardson, J.D., 1995. An extended plasma model for Saturn. J. Geophys. Res. 22, 1177–1180.

Richardson, J.D., Siscoe, G.L., 1983. The problem of cooling of the cold Io torus. J. Geophys. Res. 88, 2001–2009.

Richardson, J.D., Sittler Jr, E.C., 1990. A plasma density model for Saturn based on Voyager observations. J. Geophys. Res. 95, 12019–12031.

Richardson, J.D., Eviatar, A., McGrath, M.A., Vasyliunas, V.M., 1998. OH in Saturn's magnetosphere: observations and implications. J. Geophys. Res. 103, 20245–20255.

Saur, J., Strobel, D.F., Neubauer, F.M., 1998. Interaction of the Jovian magnetosphere with Europa: Constraints on the neutral atmosphere, J. Geophys. Res. 104, 9975.

Schreier, R., Eviatar, A., Vasyliunas, Vm, Richardson, J.D., 1993. Modeling the Europa plasma torus. J. Geophys. Res. 98, 21231–21243.

Shemansky, D.E., 1998. Neutral species in the Saturnian magnetosphere. In: Paper Presented at the 1998 WPGM Meeting, Taipei, Taiwan.

Shemansky, D.E., Hall, D.T., 1992. The distribution of atomic hydrogen in the magnetosphere of Saturn. J. Geophys. Res. 97, 4143–4161.

Shemansky, D.E., Matheson, P., Hall, D.T., Hu, H.-Y., Tripp, M., 1993. The hydroxyl radicals in the Saturnian magnetosphere. Nature 363, 329.

Shi, M., Baragiola, A., Grosjean, D.E., Johnson, R.E., Jurac, S., Schou, J., 1995. Sputtering of water ice surfaces and the production of extended neutral atmospheres. J. Geophys. Res. 100, 26387–26395.

Sittler Jr, E.C., Ogilvie, K.W., Scudder, J.D., 1983. Survey of low-energy plasma electrons in Saturn's magnetosphere: Voyager 1 and 2. J. Geophys. Res. 88, 8847–8870.

Smyth, W.H., Marconi, M., 1993. The nature of the hydrogen tori of Titan and Triton. Icarus 101, 18.

Vasyliunas, V.M., 1983. In: Dessler, A.J. (Ed.), Plasma Distribution and Flow, in Physics of the Jovian Magnetosphere. Cambridge University Press.

Wilson, G.R., Waite Jr, J.H., 1989. Kinetic modeling of the Saturn ring-ionosphere plasma environment. J. Geophys. Res. 94, 17287–17298.